0013-7227/03/$15.00/0
Printed in U.S.A.

Endocrinology 144(8):3483–3490

doi: 10.1210/en.2003-0242

Cardiac Lipid Accumulation Associated with Diastolic Dysfunction in Obese Mice

CHRISTINA CHRISTOFFERSEN, ENTELA BOLLANO, MARIE L. S. LINDEGAARD, EMIL D. BARTELS, JENS P. GOETZE, CLAUS B. ANDERSEN, AND LARS B. NIELSEN

Departments of Clinical Biochemistry (C.C., M.L.S.L., E.D.B., J.P.G., L.B.N.) and Pathology (C.B.A.), Rigshospitalet, University of Copenhagen, Copenhagen, Denmark 2100; and Department of Clinical Physiology (E.B.), Sahlgrenska University Hospital, SE-413 45 Göteborg, Sweden

Obesity may confer cardiac dysfunction due to lipid accumulation in cardiomyocytes. To test this idea, we examined whether obese *ob*/*ob* mice display heart lipid accumulation and cardiac dysfunction. *Ob*/*ob* mouse hearts had increased expression of genes mediating extracellular generation, transport across the myocyte cell membrane, intracellular transport, mitochondrial uptake, and β-oxidation of fatty acids compared with *ob*/+ mice. Accordingly, *ob*/*ob* mouse hearts contained more triglyceride (6.8 ± 0.4 *vs.* 2.3 ± 0.4 μg/mg; $P < 0.0005$) than *ob*/+ mouse hearts. Histological examinations showed marked accumulation of neutral lipid droplets within cardiac myocytes but not increased deposition of collagen between myocytes in *ob*/*ob* compared with *ob*/+ mouse hearts. On echocardiography, the ratio of E to A transmitral flow velocities (an indicator of diastolic function) was 1.8 ± 0.1 in *ob*/*ob* mice and 2.5 ± 0.1 in *ob*/+ mice ($P = 0.0001$). In contrast, the indexes of systolic function and heart brain natriuretic peptide mRNA expression were only marginally affected and unaffected, respectively, in *ob*/*ob* compared with *ob*/+ mice. The results suggest that *ob*/*ob* mouse hearts have increased expression of cardiac gene products that stimulate myocyte fatty acid uptake and triglyceride storage and accumulate neutral lipids within the cardiac myocytes. The results also suggest that the cardiac lipid accumulation is paralleled by cardiac diastolic dysfunction in *ob*/*ob* mice. (*Endocrinology* 144: 3483–3490, 2003)

OBESITY, ESPECIALLY WHEN accompanied by type II diabetes, can lead to cardiac dysfunction (1). Indeed, nonischemic heart disease constitutes the second most common cause of death in individuals with type II diabetes (2). Young diabetic individuals predominantly display diastolic cardiac dysfunction, whereas systolic heart failure in obese diabetic individuals rarely develops before middle age (3). The mechanisms involved in the precipitation of heart failure in obese diabetic individuals are, however, still not clear. It was recently proposed that an excess lipid accumulation in the diabetic cardiomyocytes could cause a lipotoxic heart disease (4, 5). In agreement with this idea, the treatment with troglitazone normalized blood glucose and insulin levels in obese diabetic *fa/fa* rats (6) and these metabolic effects were accompanied by a reduction of heart lipid stores and improvement of both systolic and diastolic cardiac function. Also, perfused hearts from obese Zucker rats display decreased cardiac output compared with control rat hearts *in vitro* (7). In lean mice, overexpression of the peroxisomal proliferator-activated receptor (PPAR)-α gene leads to lipid accumulation and deteriorated heart function (8). Streptozotocin-induced diabetes caused cardiac triglyceride accumulation and cardiac dysfunction in lean wild-type mice, whereas streptozotocin-treated diabetic apolipoprotein B (apo-B) transgenic mice had normal cardiac triglyceride levels and normal cardiac function (9). Although these studies suggest that cardiac triglyceride accumulation may be accompanied by ventricular dysfunction, the impact of obesity on cardiac lipid accumulation and the function of the mouse heart have not been investigated.

Obesity-induced type II diabetes is associated with increased plasma concentrations of free fatty acids. This presumably results in an increased delivery of fat to the heart muscle (10). However, uptake and metabolism of free fatty acids and triglycerides by cardiac myocytes can be regulated at many levels, *e.g.* hydrolysis of triglycerides in myocardial capillaries [*e.g.* by lipoprotein lipase (11)], fatty acid transport across the myocyte cell membrane [*e.g.* by CD36 (12), fatty acid transport protein (FATP) 1, and FATP 4 (13)], intracellular transport of fatty acids [*e.g.* by heart-specific fatty acid binding protein (hFABP) (14) and carnitine palmitoyl-transferase (CPT)-1 (15)], and fatty acid β-oxidation [involving a number of enzymes including long-chain acyl-coenzyme A (CoA) dehydrogenase (LCAD)]. Although the expression of several of these genes is affected in diabetic animals (14, 16–18), the relative contribution of activity changes in these pathways to lipid accumulation is not clear in the obese heart. In addition, the formation and secretion of triglycerides in apo-B-containing lipoproteins may also affect cardiac triglyceride stores (9, 19, 20). The transfer of triglycerides onto apo-B is conferred by microsomal triglyceride transfer protein (MTP) within the lumen of the endoplasmic reticulum (21). Pharmacological inhibition (22) or genetic ablation (20) of MTP activity in the heart reduces lipoprotein secretion and promotes triglyceride storage. Heart MTP gene expression

Abbreviations: apo-B, Apolipoprotein B; BNP, brain natriuretic peptide; CoA, coenzyme A; CPT, carnitine palmitoyl-transferase; DGAT, acyl CoA:diacylglycerol acyltransferase; FATP, fatty acid transport protein; GLUT-4, glucose transporter 4; hFABP, heart-specific fatty acid binding protein; LCAD, long-chain acyl-CoA dehydrogenase; LV, left ventricular; MTP, microsomal triglyceride transfer protein; Pfkm, muscle phosphofructokinase; PPAR, peroxisomal proliferator-activated receptor; SREBP, sterol regulatory element binding protein; TLC, thin layer chromatography.

levels appear to be increased in at least two settings in which the supplies of fatty acids to the myocardium exceed the utilization in β-oxidation, *i.e.* in human ischemic myocardium (19) and in streptozotocin-treated diabetic mouse hearts (9). This may reflect that an increase of the lipoprotein secretion rate acts to maintain normal (low) intracellular triglyceride levels in the cardiac myocytes.

The aim of the present study was to improve the understanding of the effects of obesity on cardiac lipid accumulation and heart function. Therefore, we characterized the lipid content in the heart, the expression of genes involved in cardiac lipid metabolism (including apo-B and MTP expression), and cardiac function in obese diabetic *ob/ob* mice and in lean nondiabetic *ob/+* control mice.

Materials and Methods

Animals

Leptin-deficient homozygous Lep^{ob}/Lep^{ob} (*ob/ob*) mice (n = 44) and heterozygote $Lep^{ob/+}$ (*ob/+*) control mice (n = 44) were obtained from M and B (Ry, Denmark), fed standard laboratory chow, and housed in temperature-controlled facilities (21–23 C) with a 12-h light, 12-h dark cycle from 0700–1900 h at the Panum Institute, Copenhagen University, or at Novo Nordisk A/S (Bagsvaerd, Denmark). The Animal Experiments Inspectorate, Ministry of Justice, Denmark, approved the study protocols. Cardiac lipids, gene expression, and cardiac function were studied in 10- to 11-wk-old female mice unless otherwise stated. The mice were killed by cervical dislocation, and the ventricular portion of the heart was immediately placed in liquid N_2 and stored at −141 C until lipid, protein, or mRNA analysis. The glucose concentration in tail blood was determined with a HUMACHECK^{Plus} glucose meter (HUMAN, Wiesbaden, Germany). Blood samples for plasma insulin measurements were collected in tubes with Na_2 EDTA, and plasma was stored at −80 C.

Histology

For electron microscopy, the neutral lipids in biopsies from the ventricular portion of the heart were stained with an imidazole-based technique (23). After Epon embedding, sections (50–70 nm) were cut with a Reichard Jung Ultra WTE 701704 microtome and inspected in a Philips 201 electron microscope. To assess cardiac fibrosis, heart biopsies from 10 *ob/ob* and 10 *ob/+* mice were fixed in 4% paraformaldehyde in 0.1 mol/liter Na_2PO_4 (pH 7.4) and embedded in paraffin. Cross-sections (5 μm) from the distal end of the ventricle of each heart were stained with Masson Trichrome. Four random digital images from each mouse were acquired with a Leica DC 300F digital camera (Leica Microsystems A/S, Herlev, Denmark). The area of blue-staining connective tissue was determined by digital image analysis using the ImageJ 1.29× freeware (http://rsb.info.nih.gov/ij). The sectioning, staining, and digital analysis of fibrosis were performed blinded with respect to mouse genotype.

Heart lipids

Lipids were extracted from approximately 30 mg of ventricular heart tissue with chloroform/methanol (24) and redissolved in toluol (1 μl/mg wet weight) for thin layer chromatography (TLC) (25). TLC plates (DC-fertigplatten SIL G-25, Macherey-Nagel, Duren, Germany; 20 × 20 cm) were impregnated with Na_2 EDTA (1 mM; pH 5.5), dried, and washed in chloroform-methanol-water (60:40:10). The plates were activated at 110 C for 30 min, and 1-μl tissue extracts and lipid standards (all lipid standards were from Sigma, Vallensbaek Strand, Denmark) with defined amounts of lipids were applied. The plates were developed in a six-step procedure (25) before being placed in 10% cupric sulfate (wt/vol) in 8% phosphoric acid (vol/vol), dried, and baked for 2 min at 200 C. Lipids in heart extract were quantified by digital image analysis. All samples were analyzed in duplicate on separate TLC plates. The precision and accuracy of this assay have been reported elsewhere (9, 24).

Gene expression

Total RNA was isolated from approximately 40 mg of heart tissue and used for cDNA synthesis and quantitative real-time PCR analysis of mRNA expression with a Lightcycler (Roche A/S, Hvidovre, Denmark) (9). The following sense and antisense primers were used: PPAR-α, 5′-aggaagccgttctgtgacat-3′ and 5′-aatcccctcctgcaacttct-3′; PPAR-γ, 5′-ggcacatctgttcttccaca-3′ and 5′-gccatcccttagttcactgg-3′; lipoprotein lipase, 5′-agggctctgcctgagttgta-3′ and 5′-agaaatttcgaaggcctggt-3′; CD36, 5′-tggagctgttattggtgcag-3′ and 5′-tgggttttgcacatcaaaga-3′; FATP 1, 5′-gcttcaacagccgtatcctc-3′ and 5′-tcttcttgttggtggcactg-3′; FATP 4, 5′-gtgttgaggtgccaggaact-3′ and 5′-tccttccgcaactctgtctt-3′; hFABP, 5′-aggtcggtagcatgaccaag-3′ and 5′-ctgcacatggatgagtttgc-3′; CPT-1, 5′-cccatgtgctcctaccagat-3′ and 5′-cgaggattctctggaactgc-3′; LCAD, 5′-ttccgggagagtgtaaggaa-3′ and 5′-tacgcttgctcttcccaagt-3′; glucose transporter 4 (GLUT-4), 5′-gctttgtggccttctttgag-3′ and 5′-caggaggacggcaaatagaa-3′; phosphofructokinase, muscle (Pfkm), 5′-gggtcactgttctgggacat-3′ and 5′-ggtcacgtcttttggtcacct-3′; and acyl CoA:diacylglycerol acyltransferase (DGAT), 5′-tcctgaattggtgtgtggtg-3′ and 5′-ggcgcttctcaatctgaaat-3′. Primer pairs for MTP, apo-B, sterol regulatory element binding proteins (SREBPs), β-actin, and brain natriuretic peptide (BNP) mRNA amplification have been reported elsewhere (9, 24). For each PCR, the specificity was assured by agarose gel electrophoresis and by DNA-sequencing of the PCR product. The relation between the time point of the log-linear increase of the fluorescence signal during the PCR and the relative concentration of an mRNA transcript was determined by parallel analyses of dilutions of a pool of liver cDNA (for MTP and apo-B) or a pool of heart cDNA (all other genes) from normal mice.

Heart microsomal triglyceride transfer activity

Extracts of microsomal proteins were prepared by homogenization of approximately 40 mg ventricular heart tissue in 1 ml buffer (50 mmol/liter Tris-HCl, 50 mmol/liter KCl, 5 mmol/liter EDTA, and protease inhibitor, Roche A/S) with a PT 1200 Polytron (Buch & Holm A/S, Herlev, Denmark). The total protein concentration in each homogenate was determined with the bicinchoninic acid protein assay (Pierce, Copenhagen, Denmark) using BSA as standard. The protein concentration was adjusted to 1.75 mg/ml, and heart homogenates were subjected to centrifugation for 60 min at 100,000 × *g* in a Beckman Optima LE-80K ultracentrifuge (Beckman Coulter Inc., Fullerton, CA). The supernatant containing the microsomal fraction was added to 1/10 volume of 0.54% sodium deoxycholate (pH 7.5) and incubated on ice for 30 min, followed by overnight dialysis at 4 C against a buffer [15 mmol/liter Tris (pH 7.4), 40 mmol/liter NaCl, 10 mmol/liter EDTA, and 0.02% NaN_3]. Triglyceride transfer activity in the microsomal protein fraction was measured at 37 C as the transfer of ^{14}C-triglycerides from labeled donor vesicles to acceptor vesicles that contained unlabeled triglycerides (26). The donor vesicles contained 40 nmol phosphatidylcholine, 0.08 nmol ^{14}C-triglyceride, 3.0 nmol cardiolipin, and 100 cpm/nmol ^{3}H- phosphatidylcholine. The acceptor vesicles contained 240 nmol phosphatidylcholine, 0.48 nmol triolein, and 100 cpm/nmol ^{3}H-phosphatidylcholine. In initial evaluations of the assay, the transfer of ^{14}C-triglycerides during 1 h increased linearly with the amount of microsomal protein extract in a range corresponding to between 0 and 125 μg of total heart protein. When donor and acceptor vesicles were incubated with microsomal proteins corresponding to 100 μg total heart protein extract, the ^{14}C-triglyceride transfer increased linearly with time for 5 h. Consequently, we measured the triglyceride transfer activity in mouse hearts by incubating the microsomal protein fraction corresponding to 100 μg of total heart protein with donor and acceptor vesicles for 4 h. The triglyceride transfer activity in each heart extract was always corrected for the transfer activity in a heat-inactivated (incubation at 65 C for 10 min) aliquot of the same extract (26) and for the spontaneous transfer between donor and acceptor vesicles in a test tube without heart extract. In each assay, we also performed parallel analysis of mouse liver microsomal extracts corresponding to 5, 10, and 20 μg total protein to assure the linearity of the assay. Samples from *ob/ob* and *ob/+* mice were always alternated, and the presented results are the mean of three determinations in separate assays.

Cardiovascular function

Systolic blood pressure and heart rate were measured in conscious mice with a computerized tail-cuff system (BP 2000, Visitech Systems, Apex, NC). For each blood pressure determination in each mouse, the result was the mean of at least one set of 10 measurements with at least nine successful readings.

Transthoracic echocardiography with Doppler flow analysis was performed in anesthetized mice with the Vived Five instrument (GE Ultrasound, Copenhagen, Denmark) and a 10-MHz transducer head. All recordings and measurements were performed by the same experienced examiner (E.B.). Left ventricular mass was calculated as $1.055 \times [(\text{LVD} + \text{PW} + \text{AW})^3 - (\text{LVD})^3]$; LVD is the left ventricular diameter in the diastolic phase, and PW and AW are the thickness of the posterior and anterior walls of the left ventricle, respectively. Anesthesia was induced with a sc injection of 0.05–0.08 ml/10 g body weight of fentanyl 0.079 mg/ml, fluanisone 2.5 mg/ml, and midazolam 1.25 mg/ml (Hypnorm/Dormicum, 1:1). In each mouse, the investigations were repeated after an ip injection of dobutamine (1 μg/g body weight).

Statistics

Differences between groups were analyzed with Student's *t* test. Welch's correction for unequal variances was used whenever appropriate. Results are expressed as mean ± SEM.

Results

Lipids in ob/ob mouse hearts

At 10–11 wk of age, female *ob/ob* mice had increased body weight (41 ± 0.7 *vs.* 20 ± 0.2 g; n = 2 × 32; $P < 0.0001$), blood glucose (13.8 ± 0.6 *vs.* 7.2 ± 0.2 mmol/liter; n = 2 × 32; $P < 0.0001$), and plasma insulin (2400 ± 208 *vs.* 120 ± 15 pmol/liter; n = 2 × 12; $P < 0.001$) as compared with *ob/+* control mice. Plasma triglyceride and free fatty acid concentrations were similar in *ob/ob and ob/+* mice (24). On electron microscopy, hearts from *ob/ob* mice contained more neutral lipid staining material within the cardiac myocytes than hearts from *ob/+* control mice (Fig. 1). Of note, we did not observe infiltration of adipocytes in the ventricular myocardium using oil-red-O staining of frozen heart sections (data not shown). To examine the lipid composition of mouse hearts, we adapted a TLC-based technique (Fig. 2A). The heart triglyceride content was 3.0-fold higher in *ob/ob* mice compared with *ob/+* mice (Fig. 2B). The heart phosphatidylcholine and phosphatidylinositol contents were also significantly higher in *ob/ob* than in *ob/+* mice, whereas the heart sphingomyelin, phosphatidylserine, phosphatidylethanoamine, cardiolipin, and unesterified cholesterol contents were similar in *ob/ob* and *ob/+* mice (Fig. 2B).

Expression of genes that affect fatty acid metabolism in ob/ob mouse hearts

The expression of genes involved in the generation of free fatty acids by lipolysis of lipoprotein triglycerides (lipoprotein lipase), fatty acid transport across the myocyte cell membrane (CD36, FATP 1, and FATP 4), intracellular transport (hFABP), mitochondrial uptake (CPT-1), and β-oxidation of fatty acids (LCAD), and diacylglycerol synthesis (DGAT) was higher in the *ob/ob* mouse hearts than in the *ob/+* mouse hearts (Fig. 3A). Genes encoding Pfkm and GLUT-4 (key regulators of glucose metabolism) were also increased in *ob/ob* compared with *ob/+* mouse hearts, whereas the expression of the PPAR-γ and PPAR-α genes was similar in the two groups (Fig. 3A).

MTP mRNA expression was increased in the *ob/ob* compared with *ob/+* mouse hearts (Fig. 3B). Apo-B mRNA expression was similar in *ob/ob* and *ob/+* mouse hearts (104 ± 25% *vs.* 100 ± 21% of the mean in *ob/+* mice; n = 2 × 10). Although a correlation between mRNA and protein expression has been indicated previously for many of the genes examined in Fig. 3A, it is unknown whether increased MTP mRNA expression in the heart also confers increased MTP protein expression. Therefore, we examine the physiological result of MTP gene expression, *i.e.* triglyceride transfer activity in heart microsomal extracts. The triglyceride transfer activity was significantly higher in the *ob/ob* than in the *ob/+* mouse hearts (Fig. 3B).

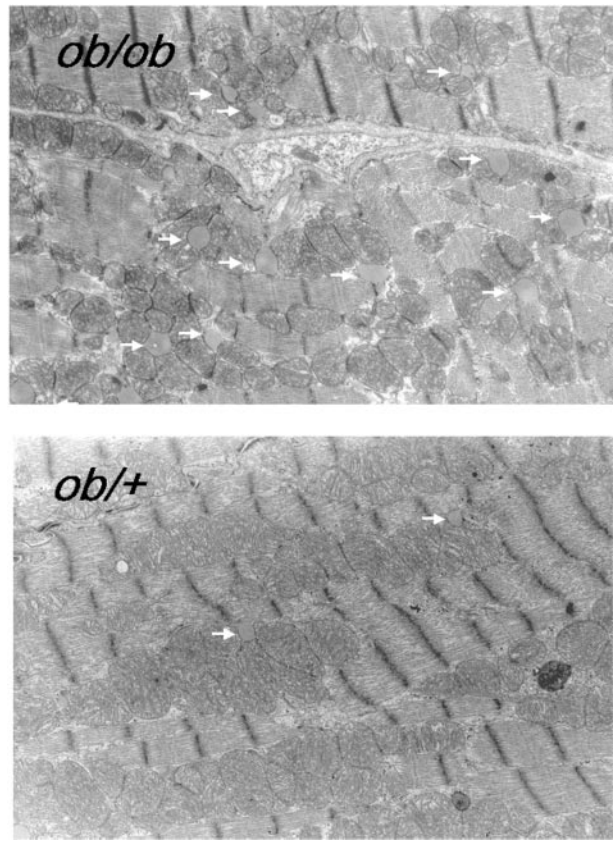

FIG. 1. Electron micrographs of *ob/ob* and *ob/+* mouse heart sections showing accumulation of neutral lipids in *ob/ob* cardiac myocytes. Neutral lipids were visualized with an imidazol-based technique. *Arrows* identify lipid droplets in myocytes. The original magnification was ×9800.

Cardiac function in ob/ob mice

Cardiac function was assessed in 10- to 11-wk-old female mice. The systolic blood pressure was approximately 10 mm Hg lower in *ob/ob* when compared with *ob/+* mice (Fig. 4A). The heart rate was lower in *ob/ob* than in *ob/+* mice in the morning, but not in the afternoon (Fig. 4B). Two previous studies have reported divergent results on the blood pressure in *ob/ob* mice. One study (27) found increased blood pressure in 6-wk-old female *ob/ob* mice during the daytime and normal blood pressure during the night using a blood pressure telemeter implanted in the left common carotid artery. The other study (28) found a lower blood pressure in 10- to 14-wk-old

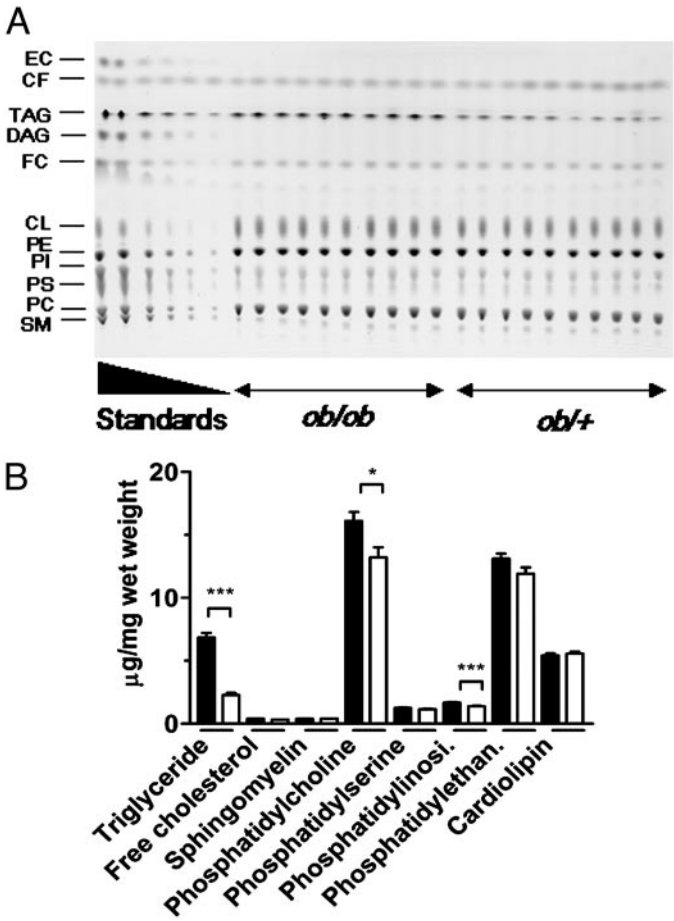

FIG. 2. Lipid composition of *ob/ob* and *ob/+* mouse hearts. A, TLC of cardiac lipids from 10 *ob/ob* and 10 *ob/+* mouse hearts and dilutions of lipid standards with known concentrations. Cardiac lipids were extracted and lipids from 1 mg of heart tissue were applied on the plate before separation and visualization, as described in *Materials and Methods*. The OD of the individual lipid spots was determined by digitalized image analysis and compared with the optical density of the standards. Whenever the OD in cardiac extracts exceeded that of the highest standard, samples were diluted and reanalyzed. An internal standard (CF) was added to assure accurate loading of samples. EC, Esterified cholesterol; CF, cholesteryl format; TAG, triglycerides; DAG, diglycerides; FC, free cholesterol; CL, cardiolipin; PE, phosphatidylethanolamine; PI, phosphatidylinositol; PS, phosphatidylserine; PC, phosphatidylcholine; SM, sphingomyelin. B, Heart lipid concentrations in *ob/ob* (*black bars*, n = 10) and *ob/+ mice (white bars,* n = 10). The results are based on duplicate TLC analysis. *, $P < 0.05$; ***, $P < 0.0005$. Values are mean ± SEM.

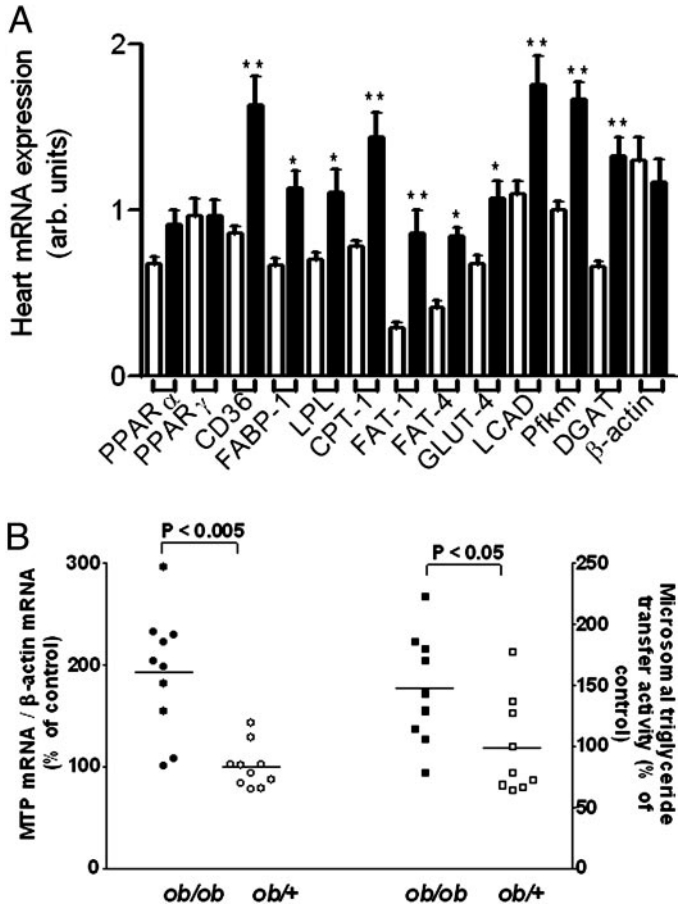

FIG. 3. Heart expression of genes affecting cardiac fatty acid metabolism and lipoprotein synthesis. A, Heart mRNA contents of the indicated genes were measured by real-time PCR in *ob/ob* (*black bars*, n = 10) and *ob/+* (*white bars*, n = 10). The mRNA expression of each gene in each sample (except the β-actin gene) was divided by the β-actin mRNA level in the same sample. The overall results were the same with and without the β-actin normalization. β-Actin mRNA is expressed as the fraction of the β-actin mRNA expression in a pool of heart cDNA from normal mice. FABP, Heart fatty acids transport protein; LPL, lipoprotein lipase; DGAT, acyl CoA:diacylglycerol acyltransferase. Values are mean ± SEM. *, $P < 0.05$; **, $P < 0.001$, after correction for multiple comparisons with the Bonferroni method. B, Heart MTP mRNA and microsomal triglyceride transfer activity in *ob/ob* and *ob/+* mice. MTP mRNA and activity were determined in different mice. Each *point* indicates values from an individual mouse. The *lines* indicate mean values. The significance levels derived from two-group comparisons are indicated *above the brackets*.

male *ob/ob* mice when the measurements were performed in darkness and blood pressure was measured with arterial catheterization. Thus, the discrepant findings might reflect differences in methodology for measuring blood pressure or the age of the mice studied.

Direct weighing of the entire heart and echocardiographic M-mode measurements of left ventricular (LV) dimensions both suggested higher heart weights in *ob/ob* than in *ob/+* mice (Table 1). Nevertheless, there was no significant difference between *ob/ob* and *ob/+* mice in the diameters of the left ventricle during systole or diastole (Table 1). To evaluate interstitial fibrosis, we stained sections of *ob/ob* and *ob/+* ventricles with Masson Trichrome and assessed the content of intercellular collagen in the ventricular portion with morphometry. The area of the blue-staining collagen was 1.0 ± 0.1% (of total area) (n = 10 in *ob/ob* mice and 0.9 ± 0.1%; n = 10 in *ob/+* mice; $P = 0.6$).

On Doppler flow analysis, parameters of LV diastolic function at baseline were markedly different in *ob/ob* mice compared with *ob/+* mice: the A-wave was 0.47 ± 0.02 m/sec in *ob/ob* mice *vs.* 0.34 ± 0.02 m/sec in *ob/+* mice ($P < 0.0005$) (Fig. 5, A and B). The E-wave was similar in *ob/ob* and *ob/+* mice (Table 1). Correspondingly, the ratio of E to A was significantly lower in *ob/ob* compared with *ob/+* mice (Table 1). LV diastolic parameters could not be evaluated after the dobutamine injection because of the high heart rates.

The echocardiographic indexes of systolic heart function

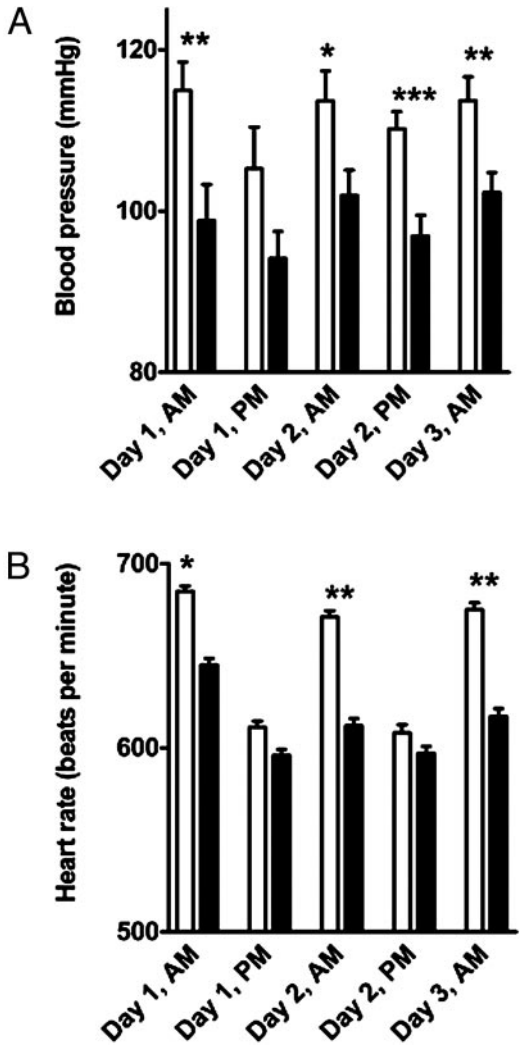

FIG. 4. Blood pressure and heart rate in conscious *ob/ob* and *ob/+* mice. A and B, Blood pressure (A) and heart rate (B) in *ob/ob* (*filled bars*, n = 12) and *ob/+* mice (*open bars*, n = 12). Blood pressure and heart rate were determined five times on 3 different days in each mouse with a digitalized tail-cuff method. AM indicates recordings made between 0830 and 1130 h, and PM indicates recordings made between 1230 and 1730 h. The light-dark cycle was from 0700–1900 h. Values are mean ± SEM. *, $P < 0.03$; **, $P < 0.008$; ***, $P < 0.0005$.

were only marginally different in *ob/ob* and in *ob/+* mice (Fig. 5C and Table 1). Fractional shortening was similar at baseline but slightly lower after dobutamine administration (1 μg/g body weight) in *ob/ob* compared with *ob/+* mice (Fig. 5C). Thus, the dobutamine-induced increase in fractional shortening was significantly smaller in *ob/ob* compared with *ob/+* mice (8.5 ± 1.5 *vs.* 17.9 ± 1.6%; $P = 0.0003$). Accordingly, dobutamine also increased the circumferential shortening to a lesser extent in *ob/ob* mice than in *ob/+* mice (4.2 ± 0.4 *vs.* 5.7 ± 0.3 circumferences/sec; $P = 0.004$) (Table 1). Of note, the effect of dobutamine on the heart rate was similar in *ob/ob* and *ob/+* mice (Table 1), indicating that the adrenergic stimulus was similar in the two groups.

The expression of BNP mRNA was similar in *ob/ob* and *ob/+* mice (Fig. 5D). Our recent studies suggest that BNP mRNA expression is a highly sensitive indicator of mild

TABLE 1. Indexes of cardiac function in *ob/ob and ob/+* mice

	ob/ob	*ob/+*
Heart weight, by weighing (mg)	97.8 ± 1.6[a]	92.4 ± 1.7
Body weight (g)	41 ± 0.7[c]	20 ± 0.3
Base line		
Heart rate (beats/min)	389 ± 11	362 ± 10
LVD (mm)	3.36 ± 0.11	3.48 ± 0.07
LVS (mm)	1.59 ± 0.05	1.43 ± 0.09
RWTH	0.60 ± 0.02	0.55 ± 0.02
Left ventricular mass, calculated (mg)	115.6 ± 5.3[b]	103.4 ± 2.6
E wave (m/sec)	0.83 ± 0.02	0.81 ± 0.01
E/A	1.81 ± 0.06[c]	2.46 ± 0.13
Deceleration time (msec)	31.0 ± 1.8	27.7 ± 1.0
Deceleration slope (m/sec^2)	28.0 ± 1.6	29.7 ± 1.2
LVOT (m/sec)	0.65 ± 0.03	0.63 ± 0.02
Emptying time (msec)	66 ± 1	65 ± 1
IVRT (msec)	24.6 ± 1.0	24.3 ± 0.9
Circumferential shortening (circ/sec)	8.9 ± 0.4	8.4 ± 0.3
After dobutamine		
Heart rate (beats/min)	569 ± 8	550 ± 11
LVOT (m/sec)	0.70 ± 0.02	0.65 ± 0.02
Circumferential shortening (circ/sec)	13.3 ± 0.3[a]	14.1 ± 0.3

Data are mean ± SEM; n = 10–12 in each group.

Echocardiography with Doppler flow analysis was performed in anesthetized mice before and after an injection of dobutamine (1 μg/g body weight). LVD and LVS are the M-mode derived diastolic and systolic diameters of the left ventricle. RWTH is the relative wall thickness. Left ventricular mass was calculated as described in *Materials and Methods*. E is the peak height of the E-wave on the mitral Doppler flow analysis. Deceleration time and slope refer to the E wave. LVOT is the left ventricular outflow tract velocity. Circumferential shortening is an integrated measure of systolic function and was calculated as (LVD − LVS)/(LVD × Emptying time). IVRT is the isovolumetric relaxation time.

[a] $P = 0.03$.
[b] $P = 0.05$.
[c] $P < 0.001$.

cardiac dysfunction in streptozotocin-treated diabetic mice (9) as in humans (29). Thus, the unchanged BNP mRNA expression supports the idea of a very mild (or no) affection of the cardiac systolic function in *ob/ob* mice.

We also examined hearts of 25-wk-old male *ob/ob* and *ob/+* mice. The heart BNP mRNA levels were similar in these *ob/ob* and *ob/+* mice [125 ± 43% (n = 12) *vs.* 100 ± 14% (n = 12) of the mean in *ob/+* mice; $P = 0.5$] despite markedly higher cardiac triglyceride concentrations in the *ob/ob* compared with *ob/+* mice (8.4 ± 2.9 *vs.* 1.7 ± 0.2 nmol/mg wet weight; $P < 0.001$).

Discussion

This study documents that leptin-deficiency-induced obesity in *ob/ob* mice is accompanied by the accumulation of triglycerides within ventricular cardiac myocytes. This is in agreement with previous findings in leptin-deficient obese *fa/fa* rats (6). The present results revealed that the contents of phosphatidylcholine and phosphatidylinositol are also increased in *ob/ob* mouse hearts. On average, the *ob/ob* hearts contained 4.5 μg more triglyceride and 3.9 μg more phosphatidylcholine per milligram wet weight than *ob/+* hearts.

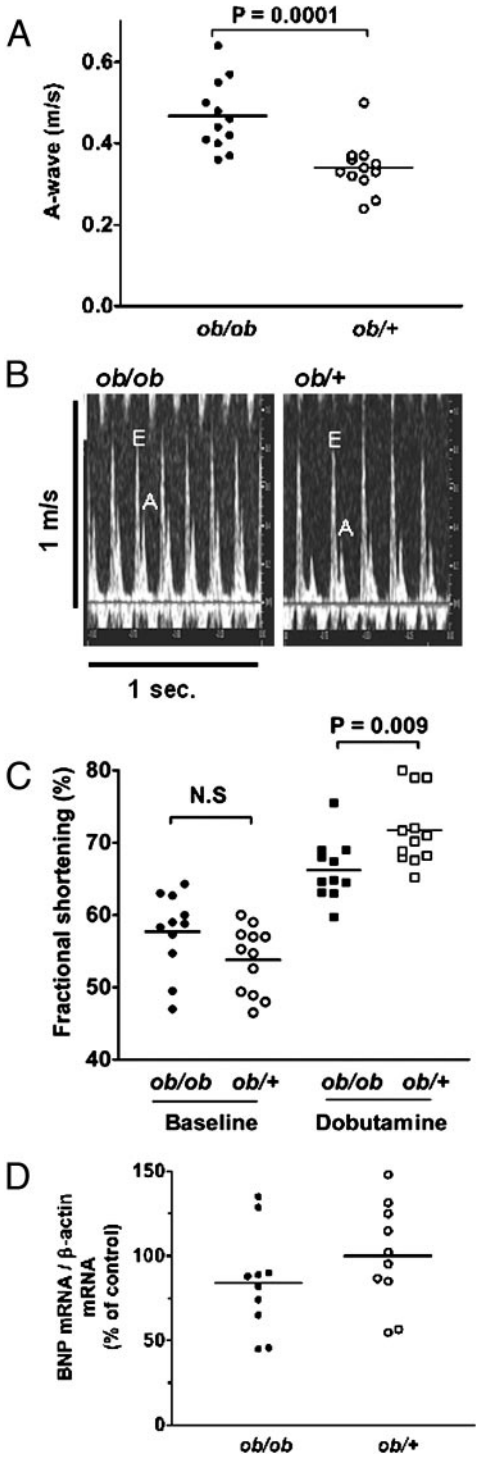

FIG. 5. Echocardiographic indexes of diastolic and systolic function and heart BNP mRNA expression in *ob/ob* and *ob/+* mice. A, A-wave in *ob/ob* and *ob/+* mice (measured as the peak height of the mitral-flow A-wave on Doppler flow recordings at baseline). Each *point* indicates values from an individual mouse. The *lines* indicate mean values. The significance level derived from the two-group comparison is indicated *above the bracket*. B, Doppler flow recordings from an *ob/ob* and an *ob/+* mouse at baseline illustrating increased peak heights of A-waves but similar peak heights of E-waves in *ob/ob* mice compared with *ob/+* mice. C, Fractional shortening at baseline and after an injection of dobutamine (measured on M-mode recordings as the difference between the diameter of the left ventricle in end-diastole and end-systole divided by the diameter in end-diastole × 100%). Each *point* indicates values from an individual mouse. The *lines* indicate mean values. The significance level derived from the two-group comparison is indicated *above the bracket*. D, Heart BNP mRNA content was determined by real-time PCR quantification in *ob/ob* (*black bars*, n = 10) and *ob/+* (*white bars*, n = 10) mice. These mice were different from those used for echocardiography. The BNP mRNA level in each sample was divided by the β-actin mRNA level in the same sample. The result was the same with and without this normalization. Results are expressed as percentage of the mean in *ob/+* mice. Each *point* indicates values from an individual mouse. The *lines* indicate mean values.

Thus, the results suggest that a significant portion of the excess fatty acids in obese mouse hearts may be stored as phosphatidylcholine. Although the physiological role of increased phospholipids in the *ob/ob* heart might simply be to store energy, the change in phospholipid levels might also affect the biomechanical function of the heart, *e.g.* through affecting Ca^{2+} -binding to the sarcolemmal membrane (30).

The plasma concentrations of free fatty acids are increased in obese type II diabetic individuals. This is believed to cause fat accumulation in muscles (10). The present study suggests that, in addition to the effect of increased plasma fatty acid concentrations, there are also changes in cardiac gene expression that promote the accumulation of free fatty acids in the cardiac myocytes. Of note, the observed changes can result from altered gene transcription rates, changes in mRNA stability, or a combination. Nevertheless, the analysis of mRNA from genes that control essential steps in myocardial fatty acid metabolism suggests that the handling of fatty acids is affected at many levels in obese diabetic mice. Thus, the results suggest that increased lipolysis in the heart (by lipoprotein lipase) increased fatty acid transport across the myocyte cell membrane (by increased expression of CD36, FATP 1, and FATP 4), and increased expression of DGAT may all participate in increasing triglyceride stores in *ob/ob* hearts. These conclusions can be further tested in the future by studying the metabolism of radiolabeled fatty acids in *ex vivo* perfused hearts.

MTP gene expression and MTP activity were increased in the *ob/ob* mouse hearts. Inasmuch as an increased MTP activity results in increased secretion of lipoprotein triglycerides from the heart [which is the case in the liver of *ob/ob* mice (24)], this result is compatible with the idea that cardiac formation of apo-B-containing lipoproteins plays a role in removing excess triglycerides from the cardiomyocytes. We previously observed that the MTP gene expression is also increased in ischemic human hearts (19) and in streptozotocin-diabetic mouse hearts (9). The present study adds further evidence to the idea that an up-regulation of MTP expression in the heart serves as a protective mechanism to unload excess lipids when the supply of fatty acids exceeds the utilization. The molecular mechanisms that lead to increased MTP gene transcription in the heart are unknown. SREBP-1 suppresses the activity of the MTP gene promoter in cultured liver (HepG2) cells (31), and we have observed a close negative correlation between SREBP-1 and MTP mRNA expression in ischemic human hearts (19). However, we did not observe differences in cardiac SREBP-1c, -1a, or -2 mRNA levels between *ob/ob* and *ob/+* control mice (data not shown). Hence, other mechanisms than altered expression of the

SREBP genes cause increased MTP expression in the *ob/ob* mouse heart.

Echocardiography with Doppler flow analysis revealed pronounced changes in the cardiac diastolic function in 11-wk-old *ob/ob* mice. An affect on diastolic function was seen as specific increases in the peak height of the A-wave and a corresponding decrease in E/A in *ob/ob* mice. This finding probably reflects impaired relaxation of the left ventricle during diastole. The type II diabetic Otsuka Long Evans Tokushima Fatty (OLETF) rat model develops diastolic cardiac dysfunction in parallel with interstitial collagen accumulation (32). In the present study, however, we could not detect a difference in interstitial collagen deposition in hearts of 10- to 11-wk-old *ob/ob* mice with diastolic dysfunction. Nevertheless, the observations of increased left ventricular mass and unchanged relative wall thickness suggested that diastolic dysfunction was paralleled by mild eccentric cardiac hypertrophy in *ob/ob* mice.

Both fractional and circumferential shortening were similar in *ob/ob* and *ob/+* mice at baseline. Moreover, the BNP mRNA expression was unaffected in 10- to 11-wk-old as well as in 25-wk-old *ob/ob* mice. These data suggest that even marked lipid accumulation in *ob/ob* mouse hearts does not lead to major cardiac systolic dysfunction, at least up to 25 wk of age. This notion is in agreement with a clinical observation that impairment of diastolic heart function precedes the impairment of systolic function by decades in human diabetic individuals (3). Conscious *ob/ob* mice had decreased blood pressure throughout the day and decreased heart rates in the morning. These findings are opposite to findings in obese human individuals, in which blood pressure is often increased (33). The lower blood pressure in *ob/ob* mice (despite pronounced obesity) might reflect decreased sympathetic drive due to the leptin deficiency (34). An increased afterload in hypertensive obese humans has been suggested as an important impetus for development of concentric cardiac hypertrophy and cardiac systolic dysfunction (35). That notion is in agreement with the present findings of unchanged indexes of systolic function in obese *ob/ob* mice without hypertension. Another possible explanation for the preserved systolic function in *ob/ob* hearts is that the toxicity of cardiac lipid accumulation only precipitates when the heart is stressed by additional stimuli, *e.g.* hypertension, cardiac ischemia, or perhaps fasting (36). That idea is equivalent to the two-hit (or more) hypothesis of lipid accumulation-associated liver damage, *i.e.* lipid accumulation in hepatocytes renders the liver more susceptible to injury by different hepato-toxins (37) and the development of steatohepatitis and cirrhosis only occurs in a subset of patients with steatosis (38). A third explanation might be that lipid-induced systolic dysfunction precipitates later than diastolic dysfunction.

The lack of overt systolic dysfunction in *ob/ob* mice, however, should be interpreted with caution because the echocardiographic measurements were performed in anesthetized mice. Although we chose two drugs with little negative inotropic effect, the anesthesia reduced the heart rate from approximately 600 bpm to approximately 400 bpm, and Semeniuk *et al.* (39) recently reported that echocardiography only detected systolic dysfunction in conscious *db/db* mice, but not in anesthetized *db/db* mice (39). Also, the contractile response to a dobutamine injection was smaller in *ob/ob* mice than in *ob/+* mice. This finding may reflect that the induced contractile response of the heart is at least partly impaired during stress in 11-wk-old *ob/ob* mice. This agrees with findings of a progressive impairment of systolic/contractile function in *db/db* mice (39) and OLETF rats (32).

Interestingly, we previously observed a normalization of heart diastolic function in mice with streptozotocin-induced diabetes when the cardiac triglyceride content was normalized by genetically increased lipoprotein secretion from the heart (9). This observation supports the principal finding of the present study, which is that neutral lipid accumulation in the *ob/ob* mouse heart primarily is associated with diastolic dysfunction. Of note, in our former study (9) the normalization of cardiac triglycerides was also accompanied by a slight improvement of systolic function.

In conclusion, obese diabetic mouse hearts display a marked increase in triglyceride content as well as an altered phospholipid composition. The increased content of neutral lipids in the heart may, at least in part, reflect increased expression of cardiac gene products that stimulate myocyte fatty acid uptake and triglyceride storage at several levels. The lipid accumulation in *ob/ob* hearts occurs despite increased MTP expression, suggesting that the capacity of local lipoprotein synthesis to prevent lipid accumulation in cardiac myocytes is exceeded in *ob/ob* mouse hearts. Echocardiography with Doppler flow analysis and measurements of cardiac BNP expression suggested that the accumulation of neutral lipids in the heart primarily is associated with diastolic dysfunction, but only discrete signs of systolic dysfunction. Thus, the precipitation of lipotoxic heart disease with systolic dysfunction is a slower process or is dependent on other factors than triglyceride accumulation *per se*.

Acknowledgments

We thank Karen Rasmussen, Lis Nielsen, Nina Broholm, and Anne Andersen for excellent technical assistance; Dr. Susanne Bro for instructions on blood pressure measurements; Dr. Claus Strom for help with echocardiography, and Dr. Bidda Rolin (Novo Nordisk A/S) for measuring plasma insulin.

Received February 24, 2003. Accepted May 5, 2003.

Address all correspondence and requests for reprints to: Lars B. Nielsen, M.D., Ph.D., D.M.Sc., Department of Clinical Biochemistry KB3011, Rigshospitalet, University of Copenhagen, Copenhagen, Denmark 2100. E-mail: larsbo@rh.dk.

This study was supported by grants from The Danish Heart Foundation, The Danish National Research Council, and The Novo Nordic Foundation for Endocrinology (to L.B.N.), and by a scholarship from Hovedstadens Sygehus Faelleskab (to C.C.).

References

1. **Alpert MA** 2001 Obesity cardiomyopathy: pathophysiology and evolution of the clinical syndrome. Am J Med Sci 321:225–236
2. **Geiss LS, Herman WH, Smith PJ** 1995 Mortality in non-insulin dependent diabetes. Diabetes in America. Bethesda, MD: National Institutes of Health; 233–257
3. **Schannwell CM, Schneppenheim M, Perings S, Plehn G, Strauer BE** 2002 Left ventricular diastolic dysfunction as an early manifestation of diabetic cardiomyopathy. Cardiology 98:33–39
4. **Unger RH** 2002 Lipotoxic diseases. Annu Rev Med 53:319–336
5. **Unger RH, Orci L** 2000 Lipotoxic diseases of nonadipose tissues in obesity. Int J Obes Relat Metab Disord 24(Suppl 4):S28–S32
6. **Zhou YT, Grayburn P, Karim A, Shimabukuro M, Higa M, Baetens D, Orci**

L, Unger RH 2000 Lipotoxic heart disease in obese rats: implications for human obesity. Proc Natl Acad Sci USA 97:1784–1789
7. **Young ME, Guthrie PH, Razeghi P, Leighton B, Abbasi S, Patil S, Youker KA, Taegtmeyer H** 2002 Impaired long-chain fatty acid oxidation and contractile dysfunction in the obese Zucker rat heart. Diabetes 51:2587–2595
8. **Finck BN, Lehman JJ, Leone TC, Welch MJ, Bennett MJ, Kovacs A, Han X, Gross RW, Kozak R, Lopaschuk GD, Kelly DP** 2002 The cardiac phenotype induced by PPARα overexpression mimics that caused by diabetes mellitus. J Clin Invest 109:121–130
9. **Nielsen LB, Bartels ED, Bollano E** 2002 Overexpression of apolipoprotein B in the heart impedes cardiac triglyceride accumulation and development of cardiac dysfunction in diabetic mice. J Biol Chem 277:27014–27020
10. **Levin K, Daa SH, Alford FP, Beck-Nielsen H** 2001 Morphometric documentation of abnormal intramyocellular fat storage and reduced glycogen in obese patients with type II diabetes. Diabetologia 44:824–833
11. **Preiss-Landl K, Zimmermann R, Hammerle G, Zechner R** 2002 Lipoprotein lipase: the regulation of tissue specific expression and its role in lipid and energy metabolism. Curr Opin Lipidol 13:471–481
12. **Coburn CT, Knapp Jr FF, Febbraio M, Beets AL, Silverstein RL, Abumrad NA** 2000 Defective uptake and utilization of long chain fatty acids in muscle and adipose tissues of CD36 knockout mice. J Biol Chem 275:32523–32529
13. **Hirsch D, Stahl A, Lodish HF** 1998 A family of fatty acid transporters conserved from mycobacterium to man. Proc Natl Acad Sci USA 95:8625–8629
14. **Schaap FG, Binas B, Danneberg H, van der Vusse GJ, Glatz JF** 1999 Impaired long-chain fatty acid utilization by cardiac myocytes isolated from mice lacking the heart-type fatty acid binding protein gene. Circ Res 85:329–337
15. **Cook GA, Park EA** 1999 Expression and regulation of carnitine palmitoyltransferase-Iα and -Iβ genes. Am J Med Sci 318:43–48
16. **Sambandam N, Abrahani MA, Craig S, Al Atar O, Jeon E, Rodrigues B** 2000 Metabolism of VLDL is increased in streptozotocin-induced diabetic rat hearts. Am J Physiol Heart Circ Physiol 278:H1874–H1882
17. **Luiken JJ, Arumugam Y, Bell RC, Calles-Escandon J, Tandon NN, Glatz JF, Bonen A** 2002 Changes in fatty acid transport and transporters are related to the severity of insulin deficiency. Am J Physiol Endocrinol Metab 283:E612–E621
18. **Engels W, van Bilsen M, Wolffenbuttel BH, van der Vusse GJ, Glatz JF** 1999 Cytochrome P450, peroxisome proliferation, and cytoplasmic fatty acid-binding protein content in liver, heart and kidney of the diabetic rat. Mol Cell Biochem 192:53–61
19. **Nielsen LB, Perko M, Arendrup H, Andersen CB** 2002 Microsomal triglyceride transfer protein gene expression and triglyceride accumulation in hypoxic human hearts. Arterioscler Thromb Vasc Biol 22:1489–1494
20. **Bjorkegren J, Veniant M, Kim SK, Withycombe SK, Wood PA, Hellerstein MK, Neese RA, Young SG** 2001 Lipoprotein secretion and triglyceride stores in the heart. J Biol Chem 276:38511–38517
21. **Shelness GS, Sellers JA** 2001 Very-low-density lipoprotein assembly and secretion. Curr Opin Lipidol 12:151–157
22. **Boren J, Veniant MM, Young SG** 1998 Apo B100-containing lipoproteins are secreted by the heart. J Clin Invest 101:1197–1202
23. **Angermuller S, Fahimi HD** 1982 Imidazole-buffered osmium tetroxide: an excellent stain for visualization of lipids in transmission electron microscopy. Histochem J 14:823–835
24. **Bartels ED, Lauritsen M, Nielsen LB** 2002 Hepatic expression of microsomal triglyceride transfer protein and in vivo secretion of triglyceride-rich lipoproteins are increased in obese diabetic mice. Diabetes 51:1233–1239
25. **Ruiz JI, Ochoa B** 1997 Quantification in the subnanomolar range of phospholipids and neutral lipids by monodimensional thin-layer chromatography and image analysis. J Lipid Res 38:1482–1489
26. **Wetterau JR, Aggerbeck LP, Bouma ME, Eisenberg C, Munck A, Hermier M, Schmitz J, Gay G, Rader DJ, Gregg RE** 1992 Absence of microsomal triglyceride transfer protein in individuals with abetalipoproteinemia. Science 258:999–1001
27. **Swoap SJ** 2001 Altered leptin signaling is sufficient, but not required, for hypotension associated with caloric restriction. Am J Physiol Heart Circ Physiol 281:H2473–H2479
28. **Mark AL, Shaffer RA, Correia ML, Morgan DA, Sigmund CD, Haynes WG** 1999 Contrasting blood pressure effects of obesity in leptin-deficient ob/ob mice and agouti yellow obese mice. J Hypertens 17:1949–1953
29. **Maisel AS, Krishnaswamy P, Nowak RM, McCord J, Hollander JE, Duc P, Omland T, Storrow AB, Abraham WT, Wu AH, Clopton P, Steg PG, Westheim A, Knudsen CW, Perez A, Kazanegra R, Herrmann HC, McCullough PA** 2002 Rapid measurement of B-type natriuretic peptide in the emergency diagnosis of heart failure. N Engl J Med 347:161–167
30. **Pierce GN, Kutryk MJ, Dhalla NS** 1983 Alterations in Ca2+ binding by and composition of the cardiac sarcolemmal membrane in chronic diabetes. Proc Natl Acad Sci USA 80:5412–5416
31. **Sato R, Miyamoto W, Inoue J, Terada T, Imanaka T, Maeda M** 1999 Sterol regulatory element-binding protein negatively regulates microsomal triglyceride transfer protein gene transcription. J Biol Chem 274:24714–24720
32. **Mizushige K, Yao L, Noma T, Kiyomoto H, Yu Y, Hosomi N, Ohmori K, Matsuo H** 2000 Alteration in left ventricular diastolic filling and accumulation of myocardial collagen at insulin-resistant prediabetic stage of a type II diabetic rat model. Circulation 101:899–907
33. **Kannel WB, Brand N, Skinner Jr JJ, Dawber TR, McNamara PM** 1967 The relation of adiposity to blood pressure and development of hypertension. The Framingham study. Ann Intern Med 67:48–59
34. **Young JB, Landsberg L** 1983 Diminished sympathetic nervous system activity in genetically obese (ob/ob) mouse. Am J Physiol 245:E148–E154
35. **Zhang R, Reisin E** 2000 Obesity-hypertension: the effects on cardiovascular and renal systems. Am J Hypertens 13:1308–1314
36. **Suzuki J, Shen WJ, Nelson BD, Selwood SP, Murphy Jr GM, Kanefara H, Takahashi S, Oida K, Miyamori I, Kraemer FB** 2002 Cardiac gene expression profile and lipid accumulation in response to starvation. Am J Physiol Endocrinol Metab 283:E94–E102
37. **Bjorkegren J, Beigneux A, Bergo MO, Maher JJ, Young SG** 2002 Blocking the secretion of hepatic very low density lipoproteins renders the liver more susceptible to toxin-induced injury. J Biol Chem 277:5476–5483
38. **Harrison SA, Diehl AM** 2002 Fat and the liver–a molecular overview. Semin Gastrointest Dis 13:3–16
39. **Semeniuk LM, Kryski AJ, Severson DL** 2002 Echocardiographic assessment of cardiac function in diabetic db/db and transgenic db/db-hGLUT4 mice. Am J Physiol Heart Circ Physiol 283:H976–H982